Letters

Modular Commutated Converter With High-Overload Capability

Biao Zhao, *Senior Member, IEEE*, Lin Wang, *Graduate Student Member, IEEE*, Xueyin Zhang, Ruihang Bai, *Graduate Student Member, IEEE*, Bin Cui, *Member, IEEE*, Lu Qu, *Member, IEEE*, Jingpeng Wu, *Senior Member, IEEE*, Zhanqing Yu, *Member, IEEE*, and Rong Zeng, *Senior Member, IEEE*

***Abstract*—This letter proposes a novel modular commutation converter with high-overload capability for high-voltage dc transmission. The combination of single-switching-device modules (SDMs) and high-switching SDMs exploits the soft-switching characteristics of the topology and the high surge-current capability of integrated gate-commutated thyristors, enabling the converter to achieve short-term high-overload capability at reduced cost and volume. The topology, operating principle, and device characteristics are presented in detail. A megawatt-level engineering prototype is developed, and experimental results demonstrate the feasibility of the proposal.**

***Index Terms*—AC–DC power conversion, high-voltage dc (HVdc), multilevel converter, overload capability.**

I. Introduction

HIGH-VOLTAGE dc (HVdc) transmission plays an increasingly significant role in large-capacity long-distance transmission, interconnection of asynchronous grids, and submarine cable transmission. With the increasing penetration of power electronic sources, the system strength and the inertia of the power system have been significantly reduced, resulting in more serious stability issues [1]. To address these challenges, the grid-connected converters will need to respond rapidly to changes in grid voltage and frequency to support the power grid. A specific level of overload capability is essential for them to provide sufficient support [2], [3].

The modular multilevel converter (MMC) has been widely applied in HVdc because of its modularity, high power quality, and flexible power control capabilities [4]. However, the number of power devices in the MMC is large due to the modular structure, and the MMC requires large capacitors for energy buffering [5]. Since the power devices in the MMC all operate in a hard-switching state under high voltage and high currents, enhancing the overload capability of the MMC must be achieved by proportionally increasing the rated capacity of the primary circuit hardware. This leads to a significant increase in the number of devices and capacitors, resulting in a huge size and extremely high cost. Several solutions have been proposed to decrease the capacitance requirement and the number of power devices [6], [7], [8]. However, all the power devices in these solutions still need to turn OFF the overcurrent during overload conditions in these topologies, meaning that the rated capacity of the primary circuit hardware also needs to be increased proportionately.

Considering the aforementioned situation, this letter proposes a novel high-overload modular commutated converter (MCC) based on integrated gate-commutated thyristors (IGCTs). The combination of single-switching-device modules (SDMs) and high-switching single-switching-device modules (HDMs) in the H-bridge leverages the soft-switching characteristics of the topology, achieving high-current turn-OFF capability with fewer power devices. By utilizing the high surge-current withstand capability of IGCTs, the short-term high-overload capability of the converter is achieved at reduced cost and volume. The topology structure, operating principle, and device characteristics are presented in detail. Finally, a 6.2-MVA prototype is built to verify the feasibility of the proposal.

II. Proposed MCC With High-Overload Capability

Fig. 1 shows the topology of the proposed MCC. It is composed of three single-phase converters connected in series on the dc side. Each single-phase converter comprises a high-switching H-bridge with cascaded submodules connected in parallel with the H-bridge dc port. The cascaded submodules consist of half- or full-bridge submodules connected in series. The high-switching H-bridge arms are composed of a high proportion of SDMs and a low proportion (about 10–20%) of HDMs connected in series.

The structures of SDM and HDM are shown in Fig. 1. The capacitor in the SDM is used to maintain voltage equalization between modules and to provide the floating power supply for the secondary circuit, and since the capacitor is not used to smooth the energy fluctuations, its capacitance is typically only a few

Received 10 October 2024; revised 21 January 2025; accepted 25 January 2025. Date of publication 28 January 2025; date of current version 30 June 2025. This work was supported by the National Key R&D Program of China under Grant 2022YFB4200800. *(Corresponding author: Rong Zeng.)*

Biao Zhao, Lin Wang, Ruihang Bai, Bin Cui, Lu Qu, Jingpeng Wu, Zhanqing Yu, and Rong Zeng are with the Department of Electrical Engineering, Tsinghua University, Beijing 100084, China (e-mail: zhao-biao@tsinghua.edu.cn; l-wang23@mails.tsinghua.edu.cn; brh20@mails.tsinghua.edu.cn; cuibin@tsinghua.edu.cn; qulu@tsinghua.edu.cn; jinpengwu@tsinghua.edu.cn; yzq@tsinghua.edu.cn; zengrong@tsinghua.edu.cn).

Xueyin Zhang is with the Tsinghua Sichuan Energy Internet Research Institute, Chengdu 610200, China (e-mail: zhangxueyin@tsinghua-eiri.org).

Color versions of one or more figures in this article are available at https://doi.org/10.1109/TPEL.2025.3535725.

Digital Object Identifier 10.1109/TPEL.2025.3535725

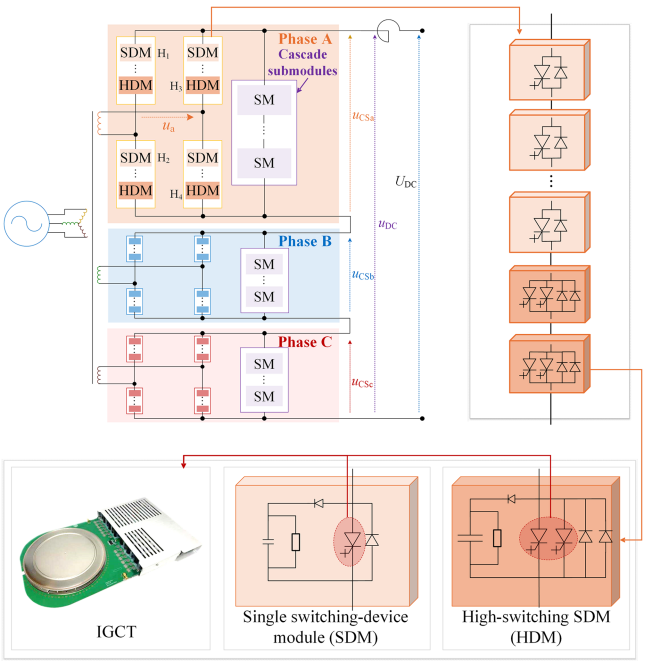

Fig. 1. MCC with high-overload capability.

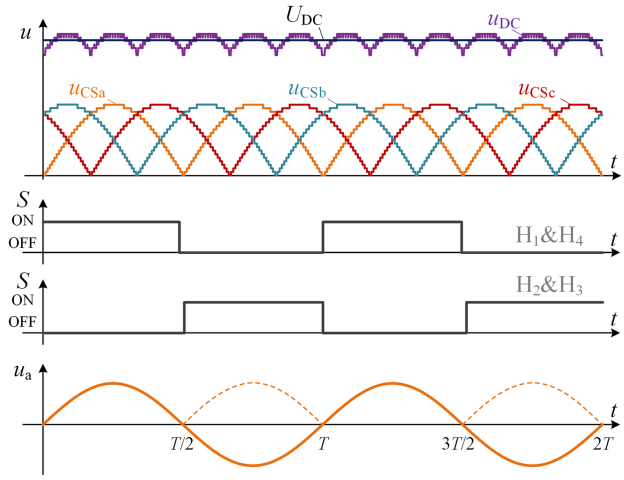

Fig. 2. Basic operating principle of AC–DC conversion in the MCC.

tens to a few hundred microfarads, which is much less than that of the capacitor in the MMC submodule. A low-current-rating auxiliary diode is used in the SDM as it only conducts the small charging current of the capacitor to replenish the costumed energy. The resistor is used for voltage equalization between SDMs in the steady state. The IGCT is selected as the switching device in the SDM. Due to the IGCT's low conduction voltage drop and high surge-current withstand capability, using IGCTs in the SDM allows for short-term overload current handling, eliminating the need for parallel devices to ensure short-term overcurrent tolerance in the SDM. This significantly reduces the number of devices and associated costs.

The topology of the HDM is the same as that of the SDM; however, it requires a higher current turn-OFF capability, referred to as "high-switching" capability. This is necessary because the HDM is responsible for achieving the turn-OFF commutation of the H-bridge, whereas the SDM does not need to turn OFF the current during operation, which will be discussed in detail in Section III. The higher current shutdown capability also indicates that the HDM has a higher current capacity. This is achieved by using devices with a higher rated current or by paralleling multiple devices in the HDM. The current capacity of the devices and the number of devices connected in parallel are determined based on the maximum turn-OFF current capability required for the overload operating conditions.

The cascaded submodules are required to use power devices with high current-switching capability or devices in parallel to ensure safe operation under overload conditions. Nevertheless, since the number of devices in the cascaded submodules is low relative to the total number of devices in the MCC, the additional cost incurred is minimal. The capacitors in the cascaded submodules also need to be increased proportionally according to the required overload multiplier. However, since the MCC's capacitance requirement is only 25% of that of the MMC [7], the increase in capacitance is significantly smaller compared to the MMC.

III. Operating Principle of the MCC

In each single-phase converter of the MCC, the cascaded submodules are modulated to generate a rectified sinusoidal voltage. The H-bridge is switched at the zero crossing of the cascaded submodule voltage, flipping the rectified sinusoid voltage to produce ac output, as shown in Fig. 2. Therefore, in normal operation, the switching frequency of the devices in HDMs and SDMs is only the power frequency. The dc ports of the three single-phase converters are directly connected in series to form the dc link. The single-phase converters are decoupled from each other and operated with a 120° phase shift between the phases to achieve three-phase ac output. In addition, the dc voltages of the three single-phase converters are interleaved and superimposed, significantly reducing the dc voltage ripple.

The key waveforms of the high-switching H-bridge arms during the commutation process are illustrated in Fig. 3(a). During operation, when the H-bridge arm needs to turn OFF a large current ($i_{\text{arm}} > 0$), the HDMs are turned OFF first at t_1. Since the voltage on the dc side of the H-bridge is zero during the commutation process, the voltage spike during switch OFF is low, and only a low proportion of HDMs is required to withstand it, while the energy from the stray inductance is absorbed by the capacitors in the HDMs. Fig. 3(b) shows the commutation process after t_1. After the dead time t_{d}, the opposite bridge arm is turned ON at time t_2. Then, one of the cascaded submodules is switched in at t_3. Finally, once the commutation process reaches a steady state, the SDMs are then controlled to turn OFF at t_4, ensuring that the IGCT in the SDM operates in a complete zero-current switching mode. The dead time of the H-bridge should be longer than the maximum possible time required for i_{arm} to decay to 0 when considering the maximum allowable turn-OFF current of the H-bridge.

This operation strategy also ensures that the diodes in the SDM operate in zero-voltage reverse recovery when $i_{\text{arm}} < 0$,

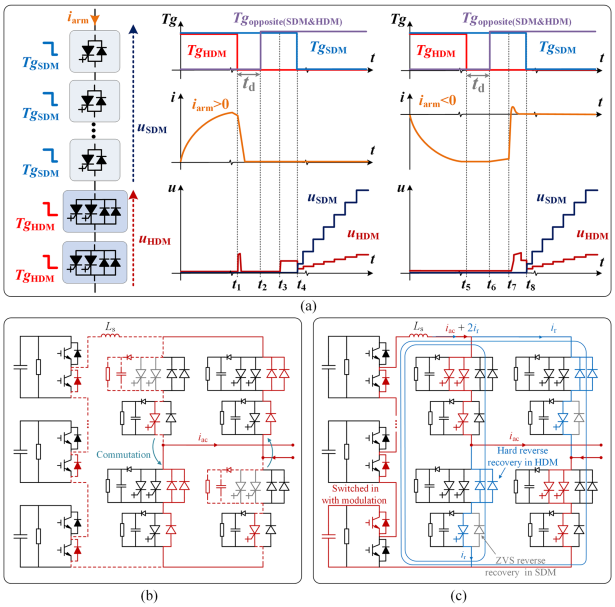

Fig. 3. Operating process of the H-bridge in the MCC. (a) Simplified key waveforms and control signals of the H-bridge. (b) Turn-OFF commutation process after t_1. (c) Reverse recovery commutation process after t_7.

as shown in Fig. 3(a). During the commutation process, the HDMs are turned OFF first at t_5. Since the bridge arm current flows through the diode, the load current does not start to commutate. After the dead time, the opposite bridge arm is turned ON at time t_6. Due to the ON-state voltage drop of the power devices, the load current begins to commutate slowly to the opposite bridge arm. Then, one of the cascaded submodules is switched in at t_7, and the voltage of the submodule causes the load current to commutate rapidly. The diodes in the HDMs undergo hard reverse recovery under the submodule voltage. For the SDMs, since the IGCTs are conducting, the diodes in the SDMs experience zero-voltage reverse recovery, significantly reducing the electrical stress, as shown in Fig. 3(c). Finally, after the commutation process reaches a steady state, the SDMs are controlled to turn OFF at t_8.

During each switching period, the energy of the capacitor in SDMs and HDMs is continuously consumed by the static voltage-sharing resistor and the auxiliary power supply, and the capacitor is charged to its rated voltage each time the voltage of cascade submodules reaches its peak, thus achieving a dynamic balancing of the internal voltage of the capacitor. The balancing of the capacitor voltages between series-connected SDMs and HDMs is ensured by the static voltage-sharing resistors connected in parallel with the capacitor.

IV. High Surge-Current Capability of the IGCT for the MCC

The SDM in the proposed MCC needs to use devices with high current capacity to ensure that it can safely withstand the significantly increased current during short-term overload operation. Fig. 4 shows the structures of IGCT and insulated gate bipolar transistor (IGBT) and a qualitative comparison of the plasma distribution in the conductive state. IGCTs are

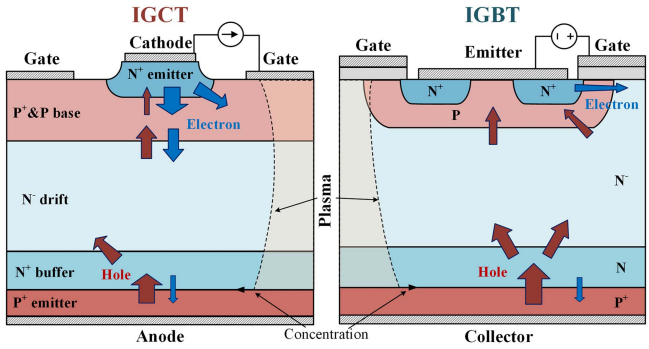

Fig. 4. Plasma distribution mechanism during conduction of the IGCT and the IGBT.

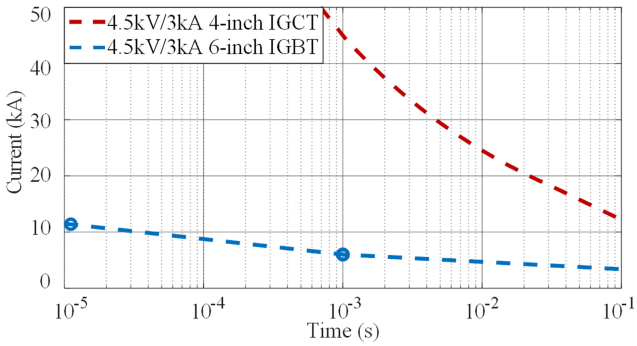

Fig. 5. Maximum allowable DC current for the IGCT and the IGBT over time.

designed with a structure similar to a thyristor. The high level of conductivity modulation within the n-drift region significantly reduces the ON-state voltage drop and supports high current densities with minimal thermal dissipation, thereby enhancing their surge-current capability. IGBTs integrate MOSFET and bipolar transistor characteristics; under a high-current conductive state, IGBTs rely on minority carrier injection into the n-drift region, which is less effective in achieving the same level of conductivity modulation as IGCTs. When subjected to surge currents, IGBTs often enter the desaturation mode, resulting in higher conduction losses and significant heating, increasing the risk of thermal runaway. These characteristics make IGCTs superior in surge-current handling capability compared to IGBTs.

Fig. 5 shows the maximum allowable dc current for 4.5-kV 3-kA 4-in IGCT (TS-ASC65L4500ID) and 6-in IGBT (5SMA3000L450300) devices over time. Limited by the desaturation effect, the IGBT device allows only 11.5 kA of short-circuit current for 10 µs. The peak collector current it permits within 1 ms is 6 kA. In contrast, the IGCT can withstand a sinusoidal half-wave surge current of 38.6-kA peak for 10 ms, with its short-term surge-current capability being more than five times that of the IGBT. The latest commercial 6-in IGCTs have maximum ratings of 4.5 kV/5.8 kA and 6.5 kV/4.3 kA. The surge-current capability of the 4.5 kV 6-in IGCT reaches up to 64-kA peak for 10 ms in a sinusoidal half-wave. Its rated capacity and surge-current withstand capability are approximately twice those of the 4-in IGCT. Currently, 4.5-kV/6-kA and 6.5-kV/5-kA

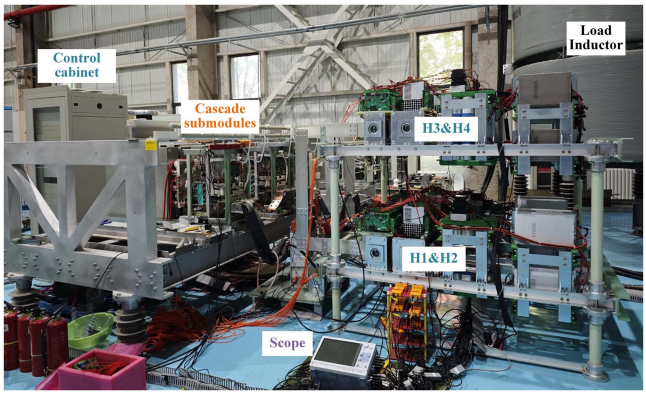

Fig. 6. MCC prototype.

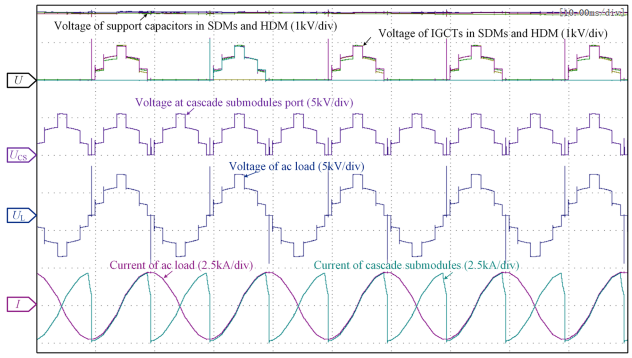

Fig. 7. Full-load power cycling experimental waveforms.

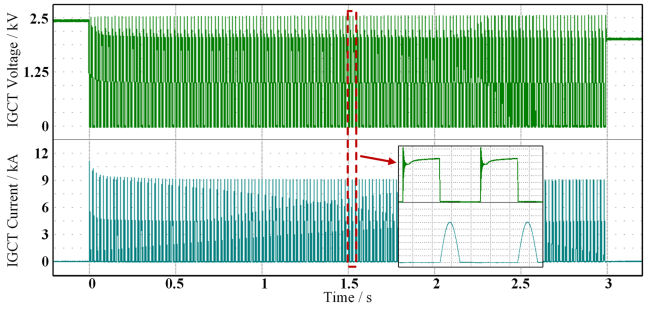

Fig. 8. Overload operation experimental waveforms of the IGCT in the SDM.

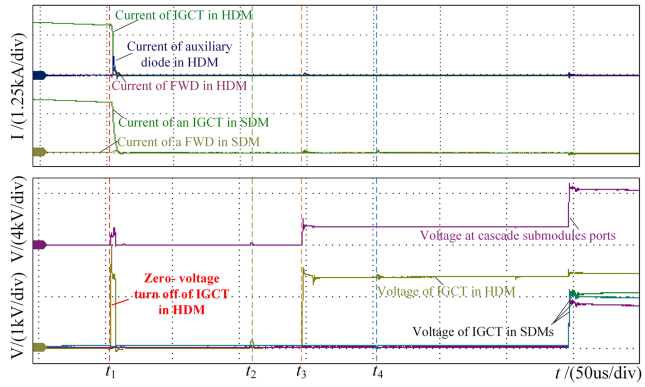

Fig. 9. Experimental results of overload operation with inductive reactive power output. The time points t_1–t_4 correspond to those in Fig. 3(a).

6-in IGCTs are under development. Based on the above, using high-surge IGCT devices in the SDM enables it to withstand the significantly increased current during short-term overload conditions without the need for excessive additional devices, thereby reducing the cost and size of the converter.

V. Megawatt-Level Engineering Prototype and Experimental Verification

To verify the feasibility of the proposed topology, a large-capacity engineering prototype with a rated capacity of 6.1 MVA was constructed. Its rated dc bus voltage is 5400 V, and the rated ac current is 1600 A, as shown in Fig. 6. Each H-bridge arm contains three SDMs and one HDM, and TS-ASC40L6500IC IGCTs are used to implement the H-bridge. Floating supply for secondary circuits and device drivers is provided by the power supply in each H-bridge module. The cascaded submodules consist of three half-bridge submodules rated at 1800 V connected in series, and TS-ASC50L4500IC IGCTs are used in submodules. All power devices are water cooled. On the dc side, a transformer with three secondary windings and three rectifier bridges was used as the converter's power supply. On the ac side, the converter is connected to an inductor as the load. Voltage and current measurements were performed using high-voltage differential probes, Rogowski coils, and a DL-950 ScopeCorder.

Fig. 7 shows the waveforms of the converter operating at full-rated power. Since a reactor was used as the load, the power output of the prototype was almost entirely reactive, and the IGCTs in the H-bridge turned OFF at the peak of the load current, approximately 2290 A. The case temperature of the IGCTs was measured using an infrared thermal imaging camera, with the highest recorded temperature being 55 °C. The prototype operated continuously at rated power for about 1.5 h, verifying its reliability.

To verify the overload capability of the prototype, an overload operation experiment was conducted, as shown in Fig. 8. The IGCTs in SDMs alternately withstood a surge current of 9-kA peak and a voltage of 2 kV without damage within 3 s. The test conditions were equivalent to the prototype delivering an overload current of 3.3 times the rated current for a short duration during an ac fault. This experiment demonstrates that the prototype has short-term high-overload capacity and confirms that the IGCTs are suitable for use in such conditions.

Fig. 9 shows the prototype operating under overload conditions, delivering inductive reactive power. Before the bridge arm turns OFF, the cascaded submodules modulate a zero-level voltage. When the IGCT in the HDM turns OFF, its voltage rises to equal the voltage of the support capacitor in the HDM, and the auxiliary diode in the HDM conducts, slightly charging the support capacitor. All IGCTs in the SDMs turn OFF at

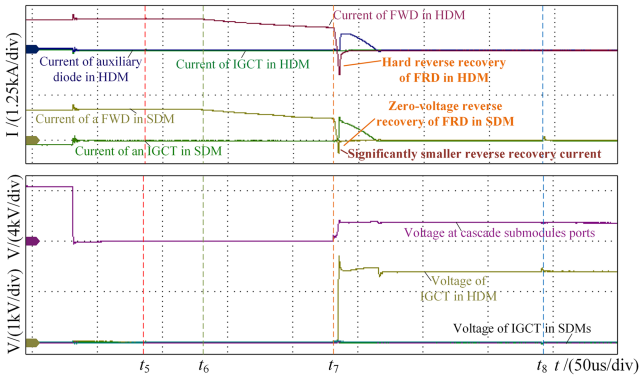

Fig. 10. Experimental results of overload operation with capacitive reactive power output. The time points t_5–t_8 correspond to those in Fig. 3(a).

zero current, experiencing significantly lower electrical stress compared to the IGCTs in the HDM.

The overload operation of the prototype while delivering capacitive reactive power is shown in Fig. 10. The cascaded submodules modulate a zero-level voltage, and the IGCT device in the HDM turns OFF, while the IGCTs in the SDMs remain ON. After the dead time, all devices in the opposite bridge arm are turned ON simultaneously. After one of the cascaded submodules is switched in again, the load current quickly commutates to the opposite bridge arm. The diode in the HDM undergoes hard reverse recovery, while in the SDM, since the IGCT remains ON, the diode undergoes zero-voltage reverse recovery, resulting in significantly lower electrical stress compared to the diode in the HDM. Finally, once the diode in the HDM completes reverse recovery, all IGCTs in the SDMs are turned OFF. These experiments verify the feasibility and effectiveness of the proposed topology and operating principle.

VI. Conclusion

This letter proposes an MCC with high-overload capability. It effectively leverages the soft-switching characteristics of the H-bridge and the strong surge-current withstand capability of IGCTs. By adopting SDMs and HDMs, the H-bridge achieves high-current turn-OFF capability with fewer device requirements, while the use of IGCTs ensures short-term overload current withstand ability. Compared with previous topologies, the proposed topology significantly reduces the number of devices and costs required to enhance the overload capability. A 6.2-MVA engineering prototype was developed, and the experimental results verify the feasibility of the proposed topology.

References

[1] J. Rocabert, A. Luna, F. Blaabjerg, and P. Rodríguez, "Control of power converters in AC microgrids," *IEEE Trans. Power Electron.*, vol. 27, no. 11, pp. 4734–4749, Nov. 2012.

[2] H. Wu and X. Wang, "Control of grid-forming VSCs: A perspective of adaptive fast/slow internal voltage source," *IEEE Trans. Power Electron.*, vol. 38, no. 8, pp. 10151–10169, Aug. 2023.

[3] J. Fang, Y. Tang, H. Li, and X. Li, "A battery/ultracapacitor hybrid energy storage system for implementing the power management of virtual synchronous generators," *IEEE Trans. Power Electron.*, vol. 33, no. 4, pp. 2820–2824, Apr. 2018.

[4] C. Zou et al., "Analysis of resonance between a VSC-HVDC converter and the AC grid," *IEEE Trans. Power Electron.*, vol. 33, no. 12, pp. 10157–10168, Dec. 2018.

[5] Y. Tang, M. Chen, and L. Ran, "A compact MMC submodule structure with reduced capacitor size using the stacked switched capacitor architecture," *IEEE Trans. Power Electron.*, vol. 31, no. 10, pp. 6920–6936, Oct. 2016.

[6] G.-J. Su, "Multilevel DC-link inverter," *IEEE Trans. Ind. Appl.*, vol. 41, no. 3, pp. 848–854, May/Jun. 2005.

[7] B. Zhao et al., "A multilevel DC-link converter for VSC-HVDC application," in *Proc. 25th Eur. Conf. Power Electron. Appl.*, Sep. 2023, pp. 1–10.

[8] R. Bai et al., "A multilevel-DC-link converter with single-device modules in series for VSC-HVDC application," *IEEE Trans. Power Electron.*, vol. 39, no. 3, pp. 3353–3364, Mar. 2024.